

Multi-Wavelength Optical Fiber Refractive Index Profiling by Spatially Resolved Fourier Transform Spectroscopy

Andrew D. Yablon

Interfiber Analysis, 26 Ridgewood Drive, Livingston, NJ 07039
andrew_yablon@interfiberanalysis.com

Abstract: We describe a non-destructive technique to measure an optical fiber's refractive index profile with sub- μm spatial resolution over a wavelength range spanning more than one octave (from 480 to 1040 nm) in a single measurement.

©2009 Optical Society of America

OCIS codes: (060.2300) Fiber measurements; (300.6300) Spectroscopy, Fourier transforms

1. Introduction

Critical fiber performance metrics, including dispersion, modal effective area, or grating spectra, are more accurately predicted with knowledge of the spectral dependence of the fiber's refractive index profile. Since most practical optical fibers are doped with a complex and proprietary mix of multiple species that may contribute to the refractive index in a non-additive way, an *in situ* method for analyzing the spectral dependence of a fiber of arbitrary composition is desirable. All previous optical fiber refractive index profiling methods [1-8] provide data at only one single probe wavelength, which is typically far outside the operating band of the fiber. Therefore, the spectral dependence of the fiber's refractive index profile can only be obtained from these methods by repeating the measurement at numerous discrete wavelengths [8]. Partly for this reason, the spectral dependence of the refractive index has only been characterized for select dopants at particular concentrations [8,9]. Furthermore, these studies either required wafer-thin fiber slices, which are inherently destructive, expensive to prepare, and permit stress relaxation, or they were performed on homogeneous bulk samples extracted from fiber preforms, which are a poor substitute for actual fiber samples since they have different thermal histories, minimal dopant diffusion, and have not experienced fiber draw. Here we describe a new, non-destructive, *in situ* technique for obtaining spectrally resolved refractive index profiles for arbitrary optical fibers across an entire octave with sub- μm spatial resolution in a single measurement. Our technique can be understood as a spatially resolved extension of Dispersive Fourier Transform Spectroscopy (DFTS) [10] and it therefore enjoys the same signal-to-noise-ratio advantage (the so-called *Multiplex* or *Fellgett Advantage*) because the brightness of a broadband probe signal scales with the bandwidth while the detector noise does not [11].

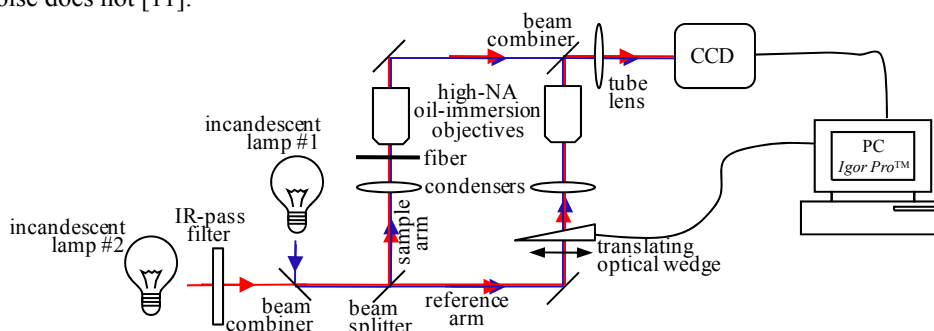


Fig. 1. Experimental Schematic

2. Experimental Setup

A schematic of the experimental setup appears in Fig. 1 and is a modification of the Transverse Interferometric Method (TIM) in which a fiber is placed in the sample arm of a Mach-Zehnder interference microscope [1,3-8]. The Michelson architecture employed by almost all Fourier transform spectrometers [10,11] has been shown to be less suitable for optical fiber measurements compared to the Mach-Zehnder configuration because substantial aberrations are incurred by double traversal of the fiber sample [1]. No cleave is necessary since the probe light travels transversely across the optical fiber [5-7], therefore the fiber could even carry a signal during the index measurement. The spatial resolution is sub-wavelength because the fiber is imaged by a high-NA (up to 1.36) oil-immersion objective lens. For the experiments described here, a Leitz interference microscope [1,5-8,12,13] was employed, although an equivalent interferometer can be constructed from conventional optical components [3,4]. A

tungsten-halogen lamp with a visible-light blocking filter was combined with an identical unfiltered lamp to yield a high-brightness incoherent wideband optical source (Fig. 2b), which avoided coherent noise effects that otherwise plague spatially resolved interferometry [6,16].

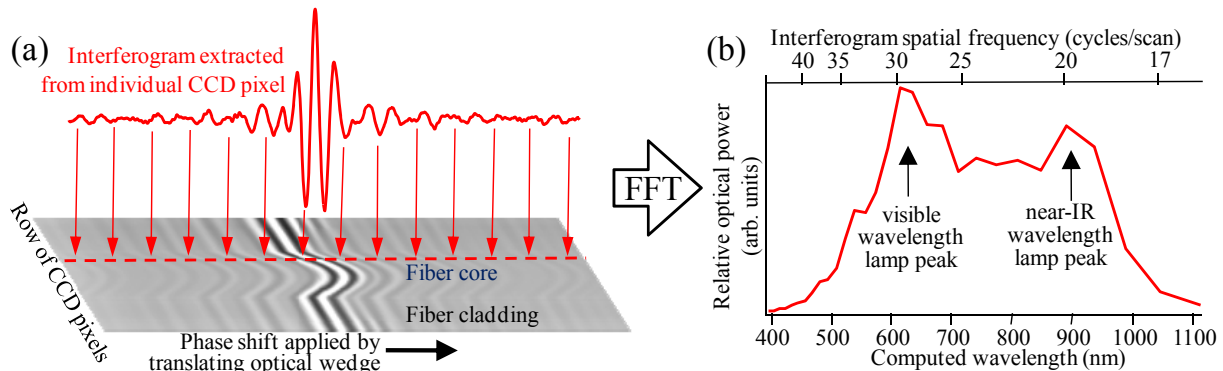


Fig. 2. Schematic illustration of data acquisition and processing showing (a) interferogram and resulting (b) power spectrum. The refractive index is determined from only the phase components of the Fourier transforms.

Traditionally, TIM required the interferometer to superpose a number of bright and dark interference fringes across a magnified image of the fiber, and the spatial deflection of these fringes would be detected and converted into a refractive index profile [1,3,5-8]. In contrast, the present method uses an optical wedge phase shifter [14] to uniformly shift the optical path length of the reference arm, thereby generating a distinct interferogram for each spatial position (pixel) in the image as a function of applied phase shift. General advantages of *phase-shifting* (or *phase-stepping*) interferometry (PSI) [4,14,15] over spatial fringe detection include: (1) robustness to fringe spacing or orientation; (2) insensitivity to illumination inhomogeneities; and (3) the opportunity to expand the field of view by stitching multiple frames together.

The detector was an analog monochrome 8-bit 640-by-480-pixel silicon CCD (*Hitachi KP160*) with excellent visible and near-IR responsivity. During a 68-second-long data acquisition scan, 2048 individual CCD frames were acquired at video rate (30 frames per second) while the continuously translating optical wedge imposed a total phase shift of about 18 μm of optical path. Data processing on a desktop PC required about 3 minutes. Both acquisition and processing were accomplished by software written in the Igor ProTM [17] environment.

Fig. 2a shows a sample interferogram obtained from a commercial graded-index multimode fiber (GI-MMF). The fast-Fourier-transform (FFT) was applied separately to each pixel location as a function of applied phase shift. Each spatial frequency in the resulting FFTs corresponded to a probe wavelength and a plot of the FFT amplitude (Fig. 2b) reveals the optical power spectrum detected by the CCD. In separate experiments, the relationship between the optical probe wavelength and the spatial frequency of the FFT was calibrated with the aid of several narrow-linewidth bandpass filters. At each optical probe wavelength, the relative phase of the FFT between the various pixels in the image reveals the optical path length variation as a function of spatial position in the image, modulo 2π . Phase ambiguities were robustly resolved using Goldstein's 2-dimensional phase unwrapping algorithms [14,15,17]. The unwrapped phase was converted into a refractive index profile at each particular optical probe wavelength using one of two methods. Axisymmetric fibers permitted the application of the inverse Abel transform [1-3,18]. Non-axisymmetric fibers, such as Polarization Maintaining (PM) fibers, were processed using a tomographic reconstruction algorithm [2,6,7,17,18] over a 180 degree range of azimuthal fiber rotation angles.

3. Results and Discussion

Despite its relatively low Δn (where $\Delta n = n - n_{\text{silica}}$), the spectral dependence of the index profile obtained from a photosensitive fiber (*Thorlabs, Inc.*) is clearly evident in Fig. 3a. Although the composition of this fiber is known only to the manufacturer, its strong spectral dependence may result from dopants intended to promote photosensitivity. Note that the spatial resolution at each wavelength is more than adequate to robustly resolve the fiber's strong central dip or *burnoff* region. Fig. 3b shows the variation of measured refractive index versus wavelength, λ , for regions of interest in several commercially available (from *Newport Corp.*, *Thorlabs Inc.*, and *Fiber Instrument Sales*) fibers. The data in Fig. 3b are normalized with respect to Δn at 660 nm (termed Δn_{660} and listed in the legend for each fiber) so that a diversity of fiber compositions can be presented with a single plot. The wavelength used by most commercial fiber and perform profilers is near 660 nm so this plot provides an estimate as to the error in Δn incurred by ignoring its spectral dependence. The curve for the GI-MMF core center agrees very well with the literature [8,9]. Not surprisingly, the high-NA fiber shows enormous spectral dependence whereas

spectral dependence of the 0.22 NA fluorine-doped cladding is surprisingly flat. The stress rod was measured in a “Panda” style PM fiber and was presumably boron-doped. To the best of our knowledge, the spectral dependence of Δn for Er-doped and Yb-doped fibers are shown for the first time in Fig. 3b and it is noteworthy that the data extends to the operating band of the Yb-doped fiber and a pump absorption band of the Er-doped fiber. Following [8], the material dispersion can be determined from the data in Fig. 3b by curve fitting followed by differentiation.

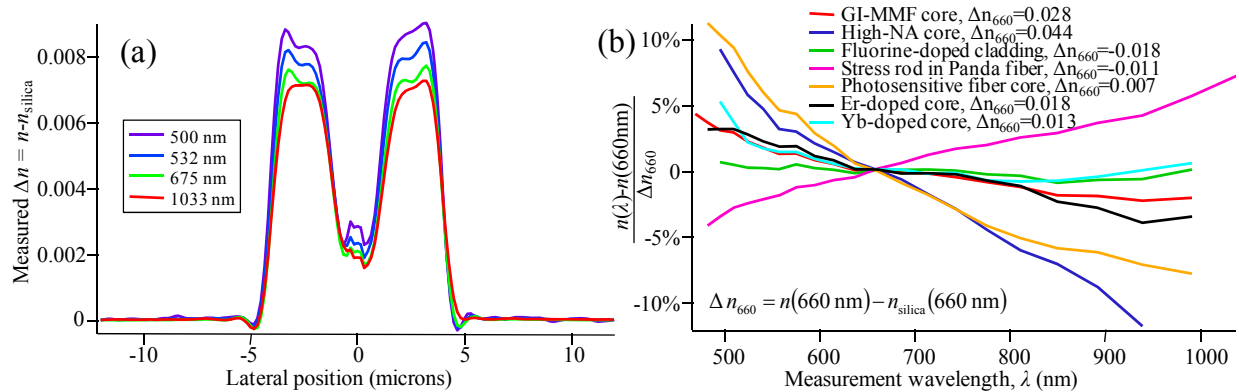


Figure 3: (a) Index profiles measured on a photosensitive fiber and (b) normalized Δn for several representative silica fiber compositions.

Instrumentation improvements could extend the capabilities demonstrated here. For example, the spectral bandwidth of these measurements was constrained by the bandwidths of the lamps and CCD as well as by the degree of chromatic correction in the imaging optics. Specially tailored optics and instrumentation could permit this technique to be applied at longer wavelengths, for example in the Er gain band, although longer wavelengths will necessarily compromise the spatial resolution. The total available optical path length shift constrained the spectral resolution of these measurements to be about 10 nm at 480 nm and about 40 nm at 1000 nm. Increasing the total applied phase shift would improve the spectral resolution and might permit the detection of interesting material dispersion characteristics in the vicinity of rare-earth absorption/emission bands. Increasing the effective dynamic range of the CCD detector beyond 8 bits would permit more accurate measurements in the vicinity of the short- and long-wavelength limits [11]. Only the phase components from the Fourier transforms were used here, but the Fourier amplitudes might be also used to measure absorption coefficients of rare-earth doped fibers in a spatially resolved fashion. The excellent spatial resolution of the technique could permit improved characterization of optical fiber gratings. This technique could also be applied to non-silica fibers (for example chalcogenide, bismuth, or polymer) by using appropriate index-matching oils. Finally, instead of measuring an optical fiber, this technique could simultaneously measure the spectral and spatial distribution of refractive index of a fluid flowing through a capillary tube or cuvette [19].

4. References

- [1] D. Marcuse, *Principles of Optical Fiber Measurement* (Academic Press, 1981), Chapter 4.
- [2] N.M. Dragomir, G.W. Baxter, and A. Roberts, “Phase-sensitive imaging techniques applied to optical fibre characterisation,” *IEE Proceedings – Optoelectronics* **153**, 217-221 (2006).
- [3] F. El-Diasty, “Characterization of optical fibres by two- and multiple-beam interferometry,” *Opt. Lasers in Eng.* **46**, 291-305 (2008).
- [4] M. Sochacka, “Optical Fibers Profiling by Phase-Stepping Transverse Interferometry,” *J Lightwave Technol* **12**, 19-23 (1994).
- [5] A.D. Yablon, *Optical Fiber Fusion Splicing* (Springer, 2005), Chapter 7.
- [6] B. Bachim, and T.K. Gaylord, “Microinterferometric optical phase tomography for measuring small, asymmetric refractive-index differences in the profiles of optical fibers and fiber devices,” *Appl. Opt.* **44**, 316-327 (2005)
- [7] B.L. Bachim, T. K. Gaylord, and S.C. Mettler, “Refractive-index profiling of azimuthally asymmetric optical fibers by microinterferometric optical phase tomography,” *Opt. Lett.* **30**, 1126-1128 (2005).
- [8] H.M. Presby and I. Kaminow, “Binary silica optical fibers: refractive index and profile dispersion measurements,” *Appl Opt* **15**, 3029 (1976).
- [9] M.J. Adams, *An Introduction to Optical Waveguides* (Wiley, 1981) pp. 244-245.
- [10] T.J. Parker, “Dispersive Fourier transform spectroscopy,” *Contemp. Physics* **31**, 335-353 (1990).
- [11] V. Saptari, *Fourier-Transform Spectroscopy Instrumentation Engineering*, (SPIE press 2003), Chapter 1.
- [12] E.C.T. Chao, *American Mineralogist* **61**, 212-228 (1976)
- [13] M. Pluta, *Advanced Light Microscopy Vol. 3* (Elsevier 1993), Chap. 16.
- [14] J. Schwider, “Advanced Evaluation Techniques in Interferometry,” in *Progress in Optics XXVIII*, E. Wolf ed. (Elsevier 1990)
- [15] H. Schreiber and J.H. Bruning, “Phase Shifting Interferometry,” in *Optical Shop Testing*, D. Malacara ed. (Wiley, 2007)
- [16] N. Warnasooriya and M. K. Kim, “LED-based multi-wavelength phase imaging interference microscopy,” *Opt. Express* **15** 9239 (2007).
- [17] Igor Pro ver. 6.10Beta, Wavemetrics, P.O. Box 2088, Lake Oswego, OR, 97035, www.wavemetrics.com
- [18] P.L. Chu and T. Whitbread, “Nondestructive determination of refractive index profile of an optical fiber: fast Fourier transform method,” *Appl. Opt.* **18**, 1117-1122 (1979).
- [19] A. Yang et al, “Measuring the refractive indices of liquids with a capillary tube interferometer,” *Appl. Opt.* **45**, 7993-7998 (2006).